# Simulations and synchrotron radiation from the relativistic jet base

O. Porth

Max-Planck-Institut für Astronomie, Königsstuhl 17, 69117 Heidelberg, Germany
e-mail: `porth@mpia.de`

**Abstract.** The central acceleration region of active galactic nuclei (AGN) is simulated for a two-component spine and sheath jet. For the steady jet component we perform the spatially resolved polarized synchrotron transfer producing observables as radio maps, spectra and derived rotation measures. The wealth of detail obtained this way helps to assess the physical processes (such as internal Faraday rotation) and model assumptions.

**Key words.** galaxies: active - galaxies: jets - ISM: jets and outflows - plasmas - polarization - radiation mechanisms: non-thermal - Radiative transfer - relativity

## 1. Introduction

The radio emission of core-dominated active galactic nuclei (AGN) is synchrotron radiation generated in a relativistic jet. Concerning the origin of the jet, several physical mechanisms are possible. In the direct vicinity of the black hole, pair creation in the disk's radiation field can fill the vacuum with a hot plasma that can be accelerated by the Blandford & Znajek (1977) process or emerge as a thermally driven coronal wind (e.g. Sauty et al., 2004). These approaches model the inner *spine* of the outflow, while a second component, the *sheath* will emerge as a relativistic magneto hydrodynamical (RMHD) wind from the innermost accretion disk as in (Porth & Fendt, 2010).

Recent (G)RMHD simulations are able to produce fast spines or funnels eventually surrounded by trans-relativistic disk winds (e.g. McKinney, 2006; Hawley & Krolik, 2006) respectively single component jets of either

*Send offprint requests to*: O. Porth

origin (e.g. Komissarov et al., 2007). In our approach, both components can be relativistic with various contributions to the total energy/mass flux.

Observations of polarization structures comparing the ridge and surrounding of Blazars, (e.g. Pushkarev et al., 2005) were initially interpreted as interactions with the surrounding medium (Attridge et al., 1999) but can also be explained by the two dynamically distinct components investigated here.

Gradients in the transverse Faraday rotation measurements (RM) of Blazar jets reveal an ordered helical field structure of the sheath assumed to be the Faraday-active medium (e.g. O'Sullivan & Gabuzda, 2009). By allowing a relativistically moving sheath, asymmetries in the RM profile can be accounted for while loosening the constraints on the viewing angle (Broderick & Loeb, 2009).

Here we present polarized radiative transfer calculations of the simulated two-component jets taking into account syn-

chrotron self-absorption and internal Faraday
rotation. The model and reference simulation
are explained in more detail in Section 2.
We describe briefly the radiative transfer
computation and intensity and RM maps in
Section 3. Our conclusions are summarized in
Section 4.

## 2. Model and reference simulation

The jet is launched from a hot corona with sub-
magnetosonic and sub-escape velocity.

## 2.1. MHD jet base model

The jet plasma follows a variable Taub equa-
tion of state utilizing a polytropic index of
$\gamma = 4/3$ for the inner component and a non-
relativistic index of $\gamma = 5/3$ for the disk-wind.
For an initially subsonic flow, it is necessary
to assign only four constant in time boundary
variables, hence for the disk wind, we provide
values for $\rho_o \propto r^{-1.5}$, $p_o \propto r^{-2.5}$, $\Omega^F \propto r^{-1.5}$
and set $E_\phi = 0$. As initial magnetic config-
uration, we apply a poloidal force free field
with $B_z \propto r^{-5/4}$. The inner component fea-
tures a solid-body rotation and constant val-
ues for $\rho_i \simeq p_i$ with relativistic tempera-
tures. In principle, the inner density should fol-
low from considerations of the pair-production
rate. However, for numerical stability reasons,
we are restricted to $\rho_i \gtrsim 0.01\max(\rho_o)$ and
adopt this value for convenience. To counter-
balance the disk rotation we added a point-
mass gravity in the origin below the domain.

## 2.2. Reference simulation

The axisymmetric initial setup is advanced in
time by the RMHD code PLUTO 3.0 (Mignone
et al., 2007). After roughly 200 inner disk ro-
tations the flow in the computational domain
settles into a quasi stationary state. In Figure 1,
we show the simulation in the $r, z$-plane after
300 inner disk rotations for a domain spanning
$300 \times 1500$ Schwarzschild radii $r_S$. This snap-
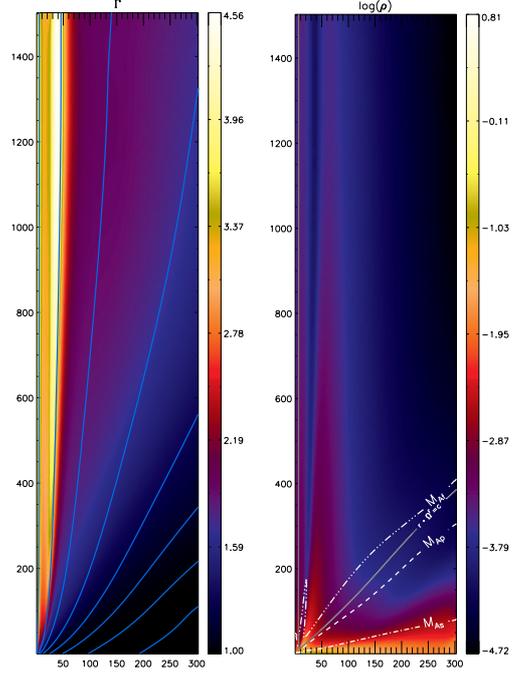shot is also taken for the radiative transfer.



**Fig. 1.** The simulations show a central hot core and
a disk wind of Lorentz factor $\Gamma \simeq 2$. A thin sheet of
$\Gamma > 4.5$ evolves at the interface. Axis labels in terms
of $r_S$ We show field-lines and characteristic surfaces
on top of the color coded Lorentz-factor (left) and
lab-frame density (right).

## 3. Stokes vector transport and radiation maps

For a continuous jet, the radiation transport
equation is most conveniently solved in the ob-
servers system (Begelman et al., 1984). We do
so for a grid of photon paths with a given di-
rection $\hat{\mathbf{n}}$.

## 3.1. Radiative transfer

The comoving emission and absorption coeffi-
cients are transformed to the common system,
resulting in the equation

$$\frac{dI_\nu}{ds} = D^{2+\alpha}\epsilon'_\nu - D^{\alpha+1.5}\kappa'_\nu I_\nu \qquad (1)$$

dependent on the Doppler factor $D(s) \equiv 1/(\Gamma(1 - \hat{\mathbf{n}} \cdot \beta))$. Considering linearly polar-

ized radiation, we solve the corresponding coupled linear equations

$$\frac{d\mathbf{I}}{ds} = \mathcal{E} - \underline{\mathbf{A}}\,\mathbf{I} \qquad (2)$$

for the three Stokes parameters $\mathbf{I} = \{I^{(l)}, I^{(r)}, U^{(lr)}\}$. We use the known rest-frame coefficients for power-law electron distributions

$$\frac{dn_e}{dE_e} = N_0 E_e^{-2\alpha-1}; \quad E_l \le E_e \le E_u \qquad (3)$$

given by Pacholczyk (1970). In the following we adopt the parameters $\gamma_l = 100$, $\gamma_u = \infty$ and $\alpha = 0.67$ to reproduce the empirical SED in the optically thin regime. Faraday rotation is calculated in accordance with Broderick & Loeb (2009); Shcherbakov (2008) by utilizing the relativistic generalization for the angle $d\chi_F$ in relation 2 .

The biggest uncertainty in synchrotron transfer is the unknown particle acceleration mechanism. Here we have to rely on posthoc assumptions that connect the electron distribution to the simulated quantities. As first approach, we express the relativistic electron number density in terms of the comoving density

$$\rho \propto N_0 \int_{E_l}^{E_u} dE_e E_e^{-2\alpha-1} \qquad (4)$$

assuming an equally efficient particle acceleration mechanism for the simulated domain and neglecting synchrotron cooling.

## 3.2. Radiation maps

The simulations are scaled to roughly match the expected values of M87, that is $M_\bullet = 6.4 \times 10^9 M_\odot$, $\dot{M}_{\mathrm{Jet}} = 10^{-5} \dot{M}_{\mathrm{Edd}}$ or alternatively $L_{\mathrm{Jet}} = 10^{44}\,\mathrm{erg/s}$. In figure 2 the intensities for several inclination angles $i$ are shown.

The maps demonstrate how the naive approach of eq. 4 promotes the dense disk-corona. For lower inclinations the inner spine is beamed to the observer. Note how the distinguished polarization structure best seen edge-on becomes obscured by beaming effects in the jet and remains unaffected in the counter-jet.
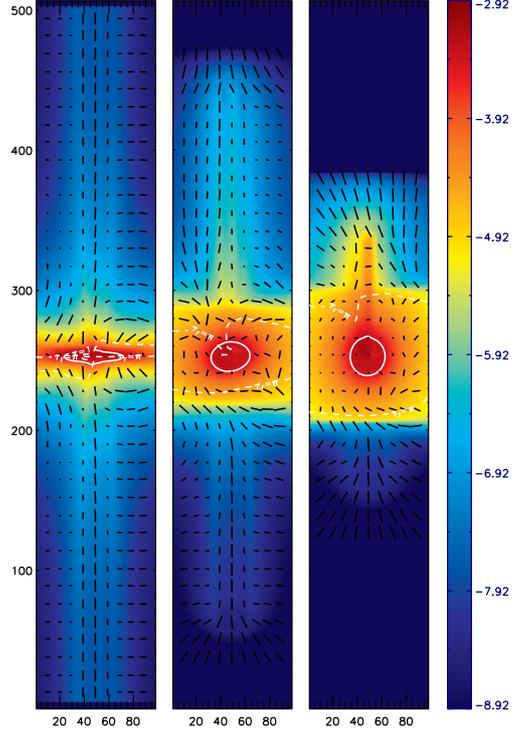


**Fig. 2.** 86GHz ideal resolution intensity maps for various inclination angles $i \in \{90°, 50°, 30°\}$. Overplotted are contours marking the loci of $\tau = 1$, $\tau_F = \pi$ and **e** polarization sticks. The x-axis extends over $420 r_S$. We obtain core-dominated maps, mainly tracing the comparatively high density and magnetic flux region of the corona. Jet rotation leads to a slight left-right asymmetry.

The low-inclination polarization is rather complex with loci of perpendicular vectors closely neighboring each other in the spine. We reckon that due to this polarization swing, an emitting volume moving in helical orbit within the spine could give rise to a variable polarization signal for BL-lac sources. Here, no change of large-scale magnetic field is required in order to explain the turn in the polarization.

## 3.3. Rotation measure

Rotation measure (RM) and spectral index maps are common diagnostics in jet observations. For our model jet, we produce these di-
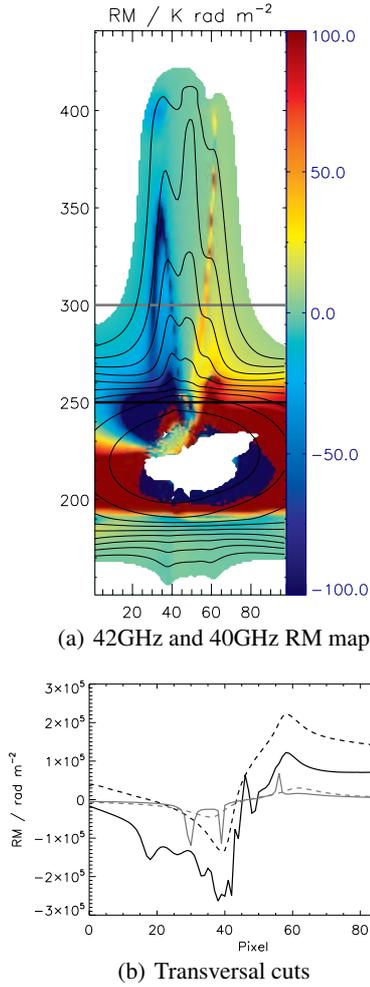
(a) 42GHz and 40GHz RM map



(b) Transversal cuts

**Fig. 3.** RM map derived from mock observations with $i = 50°$. Contours mark $I_{42\text{GHz}}$ levels in steps of ×2. Image cropped for $I < 10^{-3}I_{\max}$ and $\Pi < 1\%$. Below: Transversal cuts for the observed RM (solid) compared to the direct integration of $d\chi_F$ (dashed).

rectly out of the Stokes parameters allowing to constrain the model with the actual observables. Figure 3 gives an apparent RM map derived from

$$RM = \frac{EVPA_1 - EVPA_2}{\lambda_1^2 - \lambda_2^2}. \tag{5}$$

For comparison we also show RM cuts $\sim \int n_e \mathbf{Bdl}$. The direct integration results in a

smoother and more symmetric profile. We find that the RM appears boosted in regions of internal Faraday depolarization manifest in the spikes of the RM cuts.

## 4. Conclusions

Using high-resolution axisymmetric RMHD simulations, we showed a way to model core radiation of the inner parsec AGN jet. The dynamical simulations combined with rigorous ray-tracing reveal a wealth of detail in the observables that cannot be recovered by simplified scaling relations. An investigation that takes into account various particle acceleration recipes, resolution effects and underlying jet models will follow in a subsequent paper.

## References

Attridge, J. M., Roberts, D. H., & Wardle, J. F. C. 1999, ApJ, 518, L87

Begelman, M. C., Blandford, R. D., & Rees, M. J. 1984, Reviews of Modern Physics, 56, 255

Blandford, R. D. & Payne, D. G. 1982, MNRAS, 199, 883

Blandford, R. D. & Znajek, R. L. 1977, MNRAS, 179, 433

Broderick, A. E. & Loeb, A. 2009, ApJ, 703, L104

Hawley, J. F. & Krolik, J. H. 2006, ApJ, 641, 103

Komissarov, S. S., et al. 2007, MNRAS, 380, 51

McKinney, J. C. 2006, MNRAS, 368, 1561

Mignone, A., Bodo, G., Massaglia, S., et al. 2007, ApJS, 170, 228

O'Sullivan, S. P. & Gabuzda, D. C. 2009, MNRAS, 393, 429

Pacholczyk, A. G. 1970, Radio astrophysics (W. H. Freeman and Co)

Porth, O. & Fendt, C. 2010, ApJ, 709, 1100

Pushkarev, A. B., et al. 2005, MNRAS, 356, 859

Sauty, C., et al. 2004, Ap&SS, 293, 75

Shcherbakov, R. V. 2008, ApJ, 688, 695